

Charting the Higgs Boson Profile at e^+e^- Linear Colliders

Marco Battaglia

CERN, Geneva, Switzerland

Abstract

The problems of the origin of mass and of electro-weak symmetry breaking are central to the programme of research in particle physics, at present and in the coming decades. This paper reviews the potential of high energy, high luminosity e^+e^- linear colliders in exploring the Higgs sector, to extend and complement the data which will become available from hadron colliders. The accuracy of measurements of the Higgs boson properties will not only probe the validity of the Higgs mechanism but also provide sensitivity to New Physics beyond the Standard Model.



This paper is dedicated to Laura Alidori

1 Prologue

Explaining the origin of mass is one of the great scientific quests of our time. The Standard Model (SM), successfully tested to an unprecedented level of accuracy by the LEP, Tevatron and SLC experiments, and now also by the B -factories, addresses this question with the Higgs mechanism [1].

In this paper, I review the anticipated potential of e^+e^- linear colliders (LC) in probing the nature of the Higgs sector. As the title suggests, such studies might be compared to the efforts of explorers and cartographers, from the first sightings of new lands to the systematic charting of their coastline profiles. The first manifestation of the Higgs mechanism through the Higgs sector is the existence of at least one Higgs boson, denoted with H^0 . The observation of a new spin-0 particle would represent a first sign that the Higgs mechanism of mass generation is realised in Nature. Results of direct searches and indirect constraints, from precise electro-weak data, tell us that the Higgs boson is heavier than 114 GeV and possibly lighter than about 195 GeV [2]. We expect the Higgs boson to be first sighted by the Tevatron or the LHC, the CERN hadron collider, which will determine its mass and perform a first survey of its basic properties. Similarly to the first sighting of Hispaniola in 1492, such a discovery will represent a major breakthrough and will bring to a successful completion an intense program of experimental searches and phenomenological speculations lasting since several decades. But after the observation of a new particle with properties compatible with those expected for the Higgs boson, a significant experimental and theoretical effort will be needed to verify that the newly-discovered particle is indeed the boson of the scalar field responsible for the electro-weak symmetry breaking and the generation of mass. An e^+e^- linear collider with its well defined energy, known identity of the initial state partons, opportunity to control their helicities and a detectors which provides highly accurate information on the event properties, will promote the Higgs studies into the domain of precision physics.

2 e^+e^- collisions from beyond LEP-2 to the multi-TeV scale

The LEP-2 collider at CERN has set the highest centre-of-mass energy, reached so far in e^+e^- collisions, at $\sqrt{s}=209$ GeV. A significant further increase in both the beam energy and the luminosity has been the aim of several decades of LC designs and R&D, to advance the energy frontier in e^+e^- physics. These developments have now matured to the point where we can contemplate construction of a linear collider with initial energy

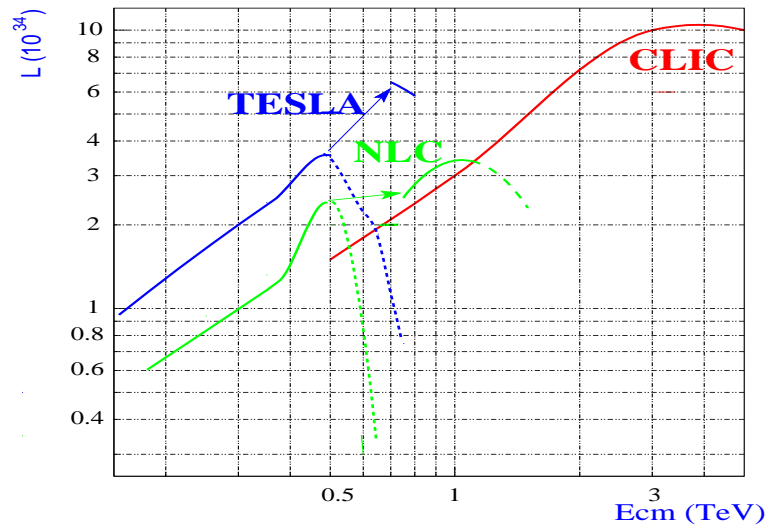


Figure 1: The design luminosity as a function of the centre-of-mass energy, \sqrt{s} , for the TESLA (SC cavities), NLC (X-band RF) and CLIC (two beam acceleration) projects. The linear collider has the potential to span its energy range over one order of magnitude. The dotted lines represent the performance for energy increases beyond 500 GeV with fixed power. The arrows show step in performance obtained by increasing the gradient (modified from [5]).

in the 500 GeV range and a credible upgrade path to ~ 1 TeV. The TESLA project [3] adopts super-conducting (SC) cavities which offer high luminosity with rather relaxed alignment requirements. As a result of a successful R&D program, gradients in excess of 23 MV/m, necessary to reach $\sqrt{s}=500$ GeV have been demonstrated. An alternative approach is taken by the NLC [4] and JLC projects which adopt X-band (11 GHz) warm cavities, evolving the concept of the SLC at SLAC, the only linear collider operated so far.

The LC energy can be later upgraded by three different strategies (see Figure 1). The first is to increase the energy at the expense of the luminosity, where the limit is set by the gradient and the available power. The second is to increase the accelerating gradient and/or adiabatically extend the active linac by adding extra accelerating structure. This scheme was successfully adopted at LEP in raising the collision energy by more than a factor of two. Here the limit is set by the site length, the achieved gradient and the RF power. Four super-conducting nine-cell cavity prototypes have been conditioned at 35 MV/m. This gradient would allow to push the TESLA \sqrt{s} energy up to 800 GeV, with a luminosity of $5.8 \times 10^{34} \text{ cm}^{-2}\text{s}^{-1}$. The NLC project aims at achieving 1 TeV, with luminosity of $3.4 \times 10^{34} \text{ cm}^{-2}\text{s}^{-1}$, by doubling the number of components and, possibly, increasing the gradient as well.

Beyond these energies, the extensions of the SC and X-band technology are more spec-

ulative. In order to attain collisions at energies in excess of 1 TeV, with high luminosity, significantly higher gradients are necessary. Also, the number of active elements in the linac must be kept low enough to ensure reliable operation. The two-beam acceleration scheme, presently being developed within the CLIC study [6] at CERN, suggests a unique opportunity to extend the physics at e^+e^- colliders to constituent energies of the order of the LHC energy frontier, and beyond. The recent test of a 30 GHz tungsten iris structure, successfully reaching an accelerating gradient of 150 MV/m [7], for a 16 ns pulse, is highly encouraging for the continuation of these studies.

3 The Neutral Higgs Boson Profile

Outlining the Higgs boson profile, through the determination of its mass, width, quantum numbers, couplings to gauge bosons and fermions and the reconstruction of the Higgs potential, stands as a greatly challenging programme. The spin, parity and charge-conjugation quantum numbers J^{PC} of Higgs bosons can be determined at the LC in a model-independent way. Already the observation of either $\gamma\gamma \rightarrow H$ production or $H \rightarrow \gamma\gamma$ decay sets $J \neq 1$ and $C = +$. The angular dependence $\frac{d\sigma_{ZH}}{d\theta} \propto \sin^2 \theta$ and the rise of the Higgs-strahlung cross section $\sigma_{ZH} \propto \beta \sim \sqrt{s - (M_H + M_Z)^2}$ allows to determine $J^P = 0^+$ and distinguish the SM Higgs from a CP -odd 0^{-+} state A^0 , or a CP -violating mixture of the two. But the LC has a unique potential for verifying that the Higgs boson does its job of providing gauge bosons, quarks and leptons with their masses. This can be obtained by testing the relation $g_{HXX} \propto M_X$ between Yukawa couplings, g_{HXX} , and the corresponding particle masses, M_X , precisely enough. It is important to ensure that the LC sensitivity extends over a wide range of Higgs boson masses and that a significant accuracy is achieved for all particle species. Here, the LC adds the precision which establishes the key elements of the Higgs mechanism, as discussed in this section and summarised in Table 1.

3.1 Couplings to Gauge Bosons

The determination of the cross-section for the $e^+e^- \rightarrow H^0 Z^0$ Higgs-strahlung process measures the Higgs coupling to the Z^0 boson and it is also a key input to extract absolute branching fractions from the experimental determination of products of production cross sections and decay rates. At the LC, the use of the di-lepton recoil mass from the $Z^0 \rightarrow \ell^+\ell^-$ decay (see Figure 2) provides a model-independent method which critically depends on the momentum resolution. An high precision central tracker and the addition of the beam-spot constraint guarantees $\Delta p/p \leq 5 \times 10^{-5} p$ (GeV/c), which is $\simeq 12$ times

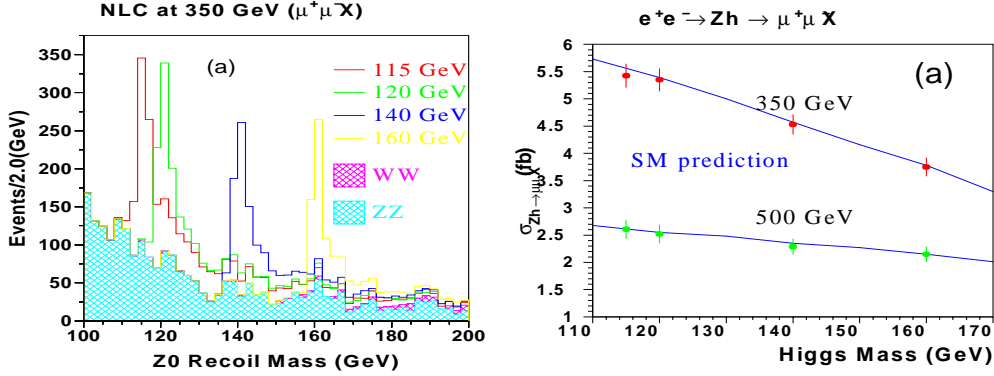


Figure 2: *Left: Di-lepton recoil mass distributions with the Higgs boson signals for different mass values. Backgrounds are superimposed. Right: evolution of the Higgs-strahlung cross section vs. M_H at $\sqrt{s}=350$ GeV and 500 GeV. The points with error bars represent the estimated uncertainties (from [10]).*

better than that obtained with the LEP detectors. At the nominal luminosity expected at $\sqrt{s}=350$ GeV, of the order of 24000 Higgs bosons would be observable in one year of operation ($= 10^7$ s), of which 4000 in a model-independent way, if $M_H=120$ GeV. A relative accuracy on the $e^+e^- \rightarrow HZ$ cross section of 2.4-3.0% can be achieved with 0.5 ab^{-1} of data at $\sqrt{s} = 350$ GeV, assuming $120 \text{ GeV} < M_H < 160$ GeV [8].

Since the recoil mass analysis is independent on the decay mode, it is also sensitive to non-standard decay modes, such as $H \rightarrow$ invisible. Several theoretical models introduce an invisible H decay width (possibly SUSY decays $\chi^0\chi^0$, but also signatures of Radion-Higgs mixing or so-called Stealth models). Such invisible Higgs decays may be problematic at hadron colliders but are detectable both indirectly, by subtracting from the total decay width the sum of visible decay modes, and directly, by analysing the system recoiling against the Z^0 in the $e^+e^- \rightarrow HZ$ process, at the LC. The direct method generally provides with a higher accuracy, corresponding to a determination of $\text{BR}(H \rightarrow \text{invisible})$ to better than 5%, so long as the invisible yield exceeds 10% of the Higgs decay width [9].

The WW -fusion reaction, $e^+e^- \rightarrow WW\nu\bar{\nu} \rightarrow H\nu\bar{\nu}$, measures the H^0 coupling to the W^\pm boson. A template analysis is based on b -tagged hadronic events at $\sqrt{s} = 350$ GeV with large missing mass and missing energy. The main background is due to the Higgs-strahlung process, when $Z^0 \rightarrow \nu\bar{\nu}$. It is possible to extract $\sigma_{H\nu\nu}$ from a χ^2 fit to the missing mass distribution, which efficiently discriminates between the two contributions [11]. Overlapping accelerator-induced $\gamma\gamma \rightarrow$ hadrons background can be suppressed by an impact parameter analysis of the forward produced particles, if the tracking resolution is small compared to the bunch length [12]. A relative accuracy of 2.6% is obtained for $M_H=120$ GeV, which becomes 10%, for $M_H=150$ GeV. However, since the branching

fraction for the $H^0 \rightarrow W^*W$ decay increases sharply in this mass interval, the accuracy on the Higgs coupling to W boson can be extracted with a small and constant uncertainties, when combining the results for production and decay processes, involving the same HWW coupling.

3.2 Couplings to Fermions

Measuring the Higgs couplings to quarks and leptons precisely is one of the main aims of Higgs studies at the LC. The requirements of such analyses have driven the concept of the innermost vertex detector and the design of the interaction region. The issue here is to measure the charged particle trajectories accurately enough to distinguish the decays $H^0 \rightarrow b\bar{b}$ from $H^0 \rightarrow c\bar{c}$, and these from $H^0 \rightarrow gg$, by reconstructing the signature decay patterns of heavy flavour hadrons. Several independent studies have been performed which indicate that the $\text{BR}(H^0 \rightarrow b\bar{b})$ can be measured to better than 3%, $\text{BR}(H^0 \rightarrow c\bar{c})$ to about 9-19% and $\text{BR}(H^0 \rightarrow gg)$ to 6-10%, if the Higgs boson is light [13–15]. The spread in the estimated accuracy for $c\bar{c}$ and gg results is attributed in terms of the different simulation and data analyses methods adopted which are currently under study. It is interesting to observe that with these experimental accuracies, the test of the coupling scaling with the fermion masses will be dominated by the present uncertainties on the latter. The case of the top quark is of special interests as it is the only fermion with an $\mathcal{O}(1)$ Yukawa coupling to the SM Higgs boson. This coupling can be measured through a determination of the cross section $e^+e^- \rightarrow t\bar{t}H^0$ [16].

Tests of the mass generation mechanism in the lepton sector are also possible by studying the decays $H^0 \rightarrow \tau^+\tau^-$ and $\mu^+\mu^-$. The τ Yukawa coupling can be measured to 2.5-5.0% using τ identification based on multiplicity and kinematics for $120 \text{ GeV} < M_H < 140 \text{ GeV}$ [13, 14]. More recently, it has been shown that also the rare decay $H^0 \rightarrow \mu\mu$ is observable at TeV-class LC and quite accurately measurable at a multi-TeV LC [17]. At 3 TeV, the relative accuracy on the muon Yukawa coupling is 3.5-10% for $120 \text{ GeV} < M_H < 150 \text{ GeV}$. This would allow to test the $g_{H\mu\mu}/g_{H\tau\tau}$ coupling ratio to a 5-8% accuracy at a multi-TeV LC, which must be compared to the 3-4% accuracy expected from combining the Muon Collider and TeV-class LC data for $120 < M_H < 140 \text{ GeV}$.

3.3 Higgs Potential

A most distinctive feature of the Higgs mechanism is the shape of the Higgs potential, $V(\Phi^*\Phi) = \lambda(\Phi^*\Phi - \frac{1}{2}v^2)^2$. In the SM, the triple Higgs coupling, g_{HHH} , is related to the Higgs mass, M_H , through the relation $g_{HHH} = \frac{3}{2} \frac{M_H^2}{v}$, where $v=246 \text{ GeV}$. By determining g_{HHH} , in the double Higgs production processes $e^+e^- \rightarrow HHZ$ and $e^+e^- \rightarrow HH\nu\nu$ [18],

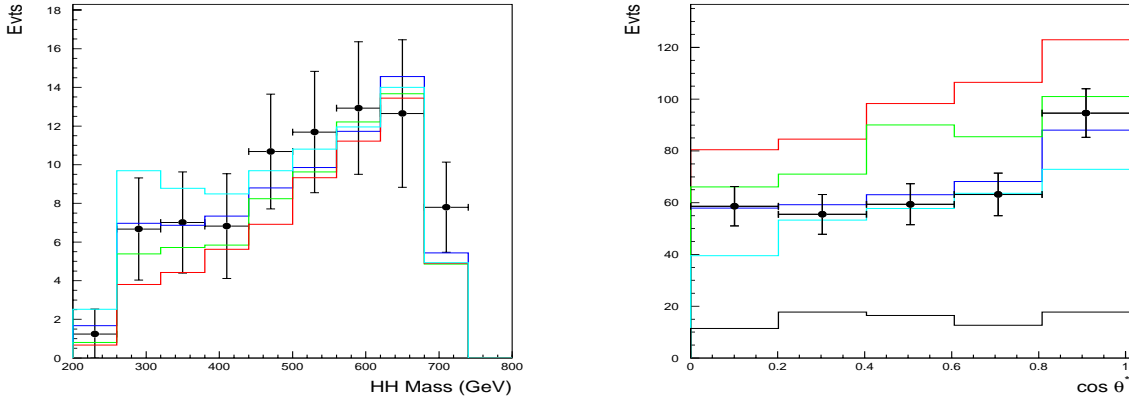


Figure 3: *Left: HH invariant mass distribution for HHZ events. Right: reconstructed $|\cos\theta^*|$ distribution for $HH\nu\bar{\nu}$ events. The lines give the expectations for $g_{HHH}/g_{HHH}^{SM} = 1.25, 1.0, 0.75$ and 0.5 . The points with error bars represent 1 ab^{-1} of SM data at $\sqrt{s}=0.8 \text{ TeV}$ and 5 ab^{-1} of SM data at $\sqrt{s}=3.0 \text{ TeV}$ respectively (from [20]).*

the above relation can be tested at the LC. These measurements are made difficult by the tiny production cross sections and the dilution due to diagrams leading to double Higgs production, but not sensitive to the triple Higgs vertex. A LC operating at $\sqrt{s} = 500 \text{ GeV}$ can measure the HHZ production cross section to about 15% accuracy, if the Higgs boson mass is 120 GeV, corresponding to a fractional accuracy of 23% on g_{HHH} [19]. Improvements can be obtained both by performing the analysis at very high energy and by introducing observables sensitive to the presence of the triple Higgs vertex (see Figure 3) [20]. On the contrary, the quartic Higgs coupling remains elusive, due to the smallness of the relevant triple Higgs production cross sections.

3.4 What if the Higgs is heavier ?

Precision electro-weak data indicate that a SM-like Higgs boson should be lighter than $\simeq 195 \text{ GeV}$. However, scenarios exist where the Higgs boson is heavier as a result of New Physics affecting the electro-weak observables. It is therefore important to assess the LC sensitivity to heavier bosons. Analyses have considered the $HZ \rightarrow \ell^+\ell^-$, $q\bar{q}$ recoil mass at 500 GeV and the $H\nu\bar{\nu}$ process at 800 GeV. In order to extract M_H , Γ_H and σ a fit to the recoil mass spectrum can be performed while the $H \rightarrow WW$ and ZZ branching fractions can be measured from the jet-jet mass in HZ [22]. The couplings to fermions are still accessible through $H \rightarrow b\bar{b}$ studied in $H\nu\bar{\nu}$. Results are summarised in Table 2.

Table 1: Summary of the accuracies on the determination of the Higgs boson profile at the LC. Results are given for a 350-500 GeV LC with $\mathcal{L}=0.5 \text{ ab}^{-1}$. Further improvements expected from a 3 TeV LC are also shown for some of the measurements.

	M_H (GeV)	$\delta(X)/X$	
		LC-500 0.5 ab^{-1}	LC-3000 5 ab^{-1}
M_H	120-180	$(3-5) \times 10^{-4}$	
Γ_{tot}	120-140	0.04-0.06	
g_{HWW}	120-160	0.01-0.03	
g_{HZZ}	120-160	0.01-0.02	
g_{Htt}	120-140	0.02-0.06	
g_{Hbb}	120-160	0.01-0.03	
g_{Hcc}	120-140	0.03-0.10	
$g_{H\tau\tau}$	120-140	0.03-0.05	
$g_{H\mu\mu}$	120-140	0.15 0.04-0.06	
CP test	120	0.03	
g_{HHH}	120-180	0.20 - - 0.07-0.09	

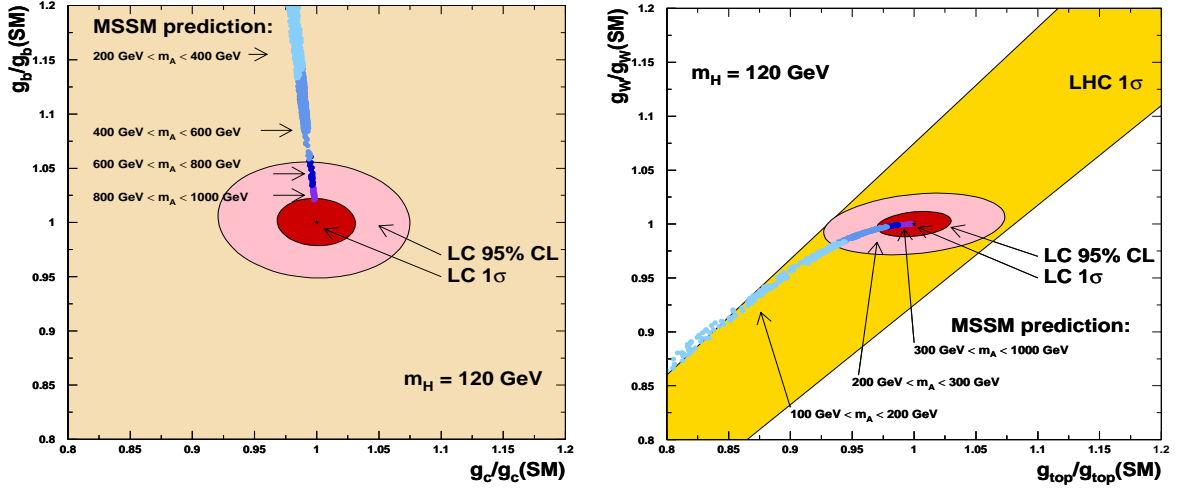


Figure 4: Expected accuracies on the Higgs couplings from a global fit to the cross section and branching fraction determinations at the LC. Left: g_{Hbb} vs. g_{Hcc} and Right: g_{HWW} vs. g_{Htt} . Couplings are normalised to their SM predictions. The expected MSSM values are also shown for different values of M_A . Contours show the 1 σ and the 95% C.L. regions. The band on the right reproduces the expected sensitivity of the LHC data (from [21]).

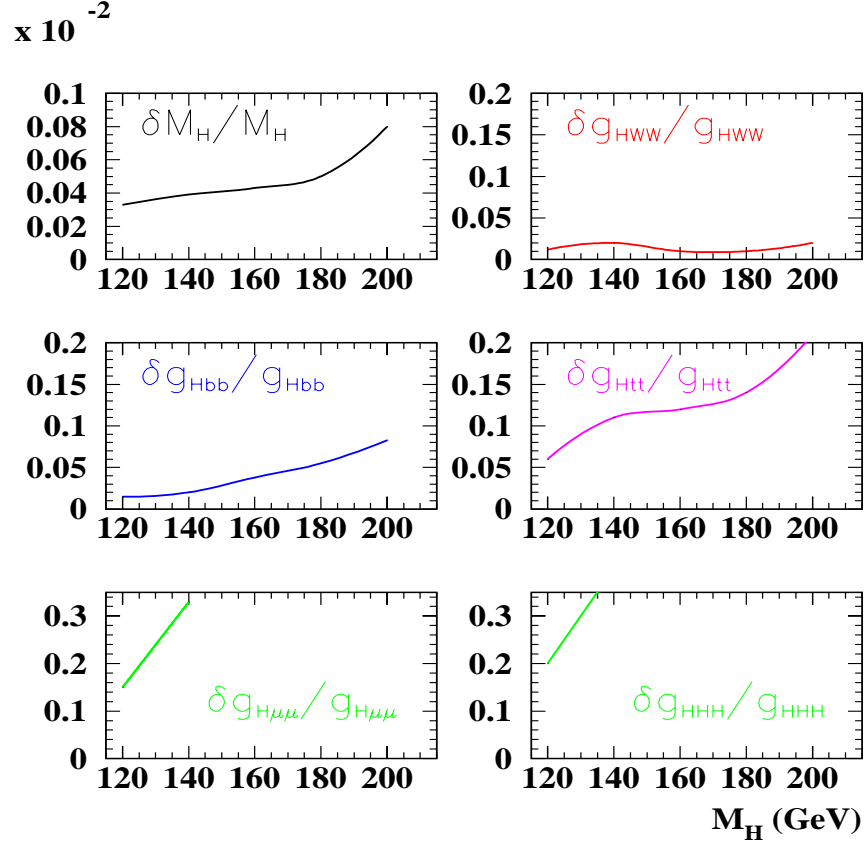


Figure 5: Anticipated accuracies for the determination of the main Higgs properties at the LC, for $\sqrt{s} = 350 - 800$ GeV, as a function of the Higgs boson mass.

Table 2: Summary of the accuracies on the determination of a heavy Higgs boson profile at the LC. Results are given for a 500-800 GeV LC with $\mathcal{L}=0.5$ and 1.0 ab^{-1} . Further improvements expected from a 3 TeV LC are also shown for some of the measurements.

	M_H GeV	$\delta X/X$	
		LC-500/800 0.5/1 ab^{-1}	LC-3000 5 ab^{-1}
M_H	240	9×10^{-4}	
Γ_H	240	0.12	
$\sigma(e^+e^- \rightarrow HZ)$	240	0.04	
$\text{BR}(H \rightarrow ZZ)$	240	0.10	
$\text{BR}(H \rightarrow WW)$	240	0.07	
$\text{BR}(H \rightarrow b\bar{b})$	200	0.16 0.04	
$\text{BR}(H \rightarrow b\bar{b})$	220	0.27 0.05	

4 An Extended Higgs Sector

Despite its successful tests, the Standard Model must be embedded into a more fundamental theory valid at higher energies, in order to explain its many parameters and cure remaining problems, such as the stabilisation of the Higgs potential. Supersymmetry is the simplest perturbative explanation for low-scale electroweak symmetry breaking, and, in its minimal realization (MSSM), predicts that the lightest Higgs boson must be lighter than about 130 GeV. In the MSSM, as in more general 2HDM extensions of the SM, the Higgs sector consists of two doublets, generating five physical Higgs states: h^0 , H^0 , A^0 and H^\pm . The h^0 and H^0 states are CP even while the A^0 is CP odd. The masses of the CP-odd Higgs boson, M_A , and the ratio of the vacuum expectation values of the two doublets $\tan\beta = v_2/v_1$ are free parameters. The study of the lightest neutral MSSM Higgs

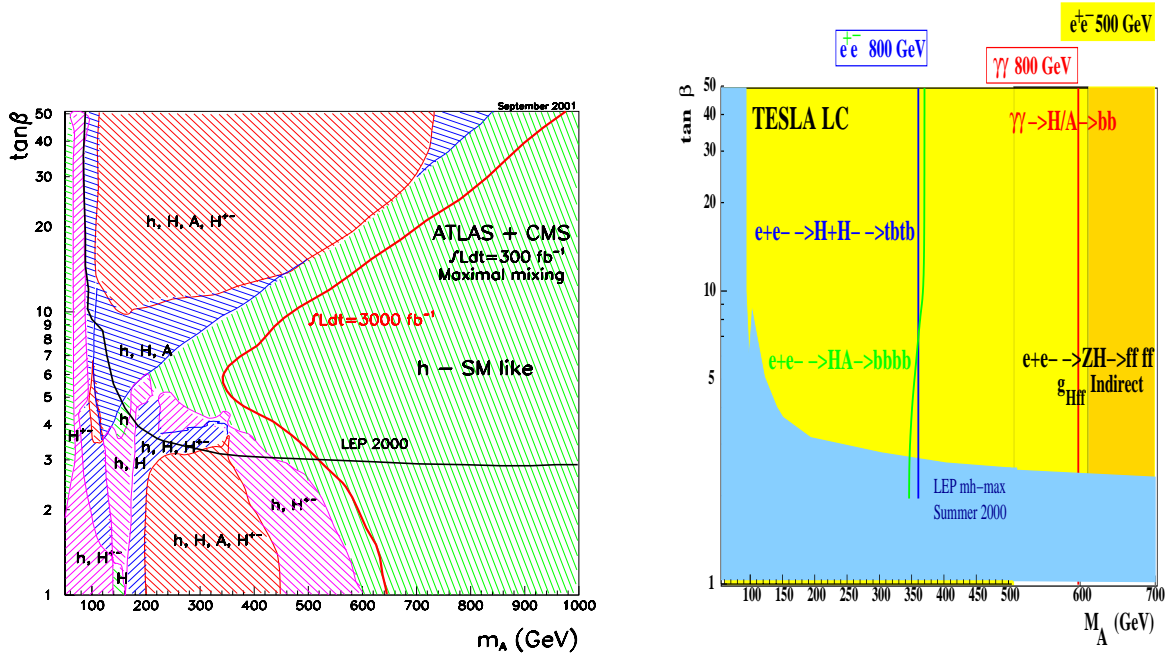


Figure 6: Reach for MSSM Higgs boson discovery in the M_A - $\tan\beta$ plane at LHC and LC. Left: expected combined performance of ATLAS and CMS with $\mathcal{L}=300 \text{ fb}^{-1}$. The wedge at large M_A and moderate $\tan\beta$ values corresponds to the parameter region where only the lightest Higgs is observable. Right: expected LC performance at $\sqrt{s}=500$ and 800 GeV . The direct search extends up to $M_A \simeq 350 \text{ GeV}$, while the indirect sensitivity extends to M_A values of $600\text{--}700 \text{ GeV}$. A $\gamma\gamma$ collider with $\sqrt{s_{ee}}=800 \text{ GeV}$ should match this limit with the direct observation of single H^0 and A^0 production.

boson, h^0 , follows closely that of the SM H discussed above and those results remain in general valid. The mass and coupling patterns of the other bosons vary with the model parameters. However, in the decoupling limit the H^\pm , H^0 and A^0 bosons are expected

to be heavy and to decay predominantly into quarks of the third generation. Establishing their existence and determining their masses and main decay modes, through their pair production $e^+e^- \rightarrow H^0 A^0$ and $H^+ H^-$ would represent a decisive step in the understanding of the Higgs sector, which will most probably require extended LC operations at $\sqrt{s} \geq 500$ GeV.

4.1 Indirect Sensitivity

The precision study of the Higgs couplings to fermions and gauge bosons may already reveal its SM or Supersymmetric nature, before the direct observation of heavier bosons. In fact, in the SM we expect the ratios of Yukawa couplings to be proportional to those of the particle masses. On the contrary, in Supersymmetry, couplings to up-like and down-like fermions are shifted w.r.t. their SM predictions as $\frac{BR(h \rightarrow f_u \bar{f}_u)}{BR(h \rightarrow f_d \bar{f}_d)} \propto \frac{1}{\tan^2 \alpha \tan^2 \beta} \simeq \frac{(M_h^2 - M_A^2)^2}{(M_Z^2 + M_A^2)^2}$. This can be exploited to distinguish the SM H^0 from the Supersymmetric h^0 with precise determination of its couplings (see Figure 4). If they would result to be incompatible with those predicted by the SM, informations can be extracted on the value of the A^0 mass, M_A , which is a fundamental parameter in Supersymmetry. Several analyses of the indirect sensitivity to the MSSM provided by the accurate determination of the Higgs couplings have been conducted as a function of M_A . Results show consistently that for $M_A < 650$ GeV, the MSSM h^0 can be distinguished from the SM H^0 , mostly from its $b\bar{b}$, $c\bar{c}$ and WW couplings (see Figure 6). Furthermore, SUSY sbottom-gluino and stop-higgsino loops may shift the effective b -quark mass in the hbb couplings: $\Delta m_b \propto \mu M_{\tilde{g}} \tan \beta f(M_{\tilde{b}_1}, M_{\tilde{b}_2}, M_{\tilde{g}})$. This becomes important in specific regions of the parameter space, at large $\tan \beta$ and small M_A values, where the $b\bar{b}$ coupling can be dramatically suppressed. These effects can be accurately surveyed at the LC.

4.2 Direct Sensitivity

If the heavy Higgs bosons are above pair-production threshold, the $e^+e^- \rightarrow H^0$, $A^0 \rightarrow b\bar{b}$, $e^+e^- \rightarrow H^+ \rightarrow t\bar{b}$ or $H^+ \rightarrow W^+ h^0$, $h^0 \rightarrow b\bar{b}$ processes will provide with very distinctive, yet challenging, multi-jet final states with multiple b -quark jets, which must be efficiently identified and reconstructed. Example analyses have shown that an accuracy of about 0.3% on the boson masses and of $\simeq 10\%$ on the product $\sigma \times BR$ can be obtained at the LC [23, 24].

In addition, the $\gamma\gamma \rightarrow A^0$ and H^0 process at the $\gamma\gamma$ collider, is characterised by a sizable cross section which may probe the heavier part of the Higgs spectrum, beyond the e^+e^- reach. Finally, a scan of the A^0 and H^0 thresholds at the $\gamma\gamma$ collider can in principle

resolve a moderate $A^0 - H^0$ mass splitting [25,26], which could not otherwise be observed at other colliders.

4.3 CP violation

Extensions of the SM may introduce new sources of CP violation, through additional physical phases whose effects can be searched for in the Higgs sector. Supersymmetric one-loop contributions can lead to differences in the decay rates of $H^+ \rightarrow t\bar{b}$ and $H^- \rightarrow t\bar{b}$, in the MSSM with complex parameters [27]. This CP asymmetry is expressed as $\delta CP = \frac{\Gamma(H^- \rightarrow t\bar{b}) - \Gamma(H^+ \rightarrow t\bar{b})}{\Gamma(H^- \rightarrow t\bar{b}) + \Gamma(H^+ \rightarrow t\bar{b})}$ and it can amount to up to $\simeq 15\%$. As the leading contributions come from loops with \tilde{t} , \tilde{b} and \tilde{g} , δCP is sensitive to these parameters. With the expected statistics of $e^+e^- \rightarrow H^+H^- \rightarrow t\bar{b}t\bar{b}$ at $\sqrt{s}=3$ TeV and assuming realistic charge tagging performances, a 3σ effect for $\mathcal{L}=5$ ab^{-1} would be observed for an asymmetry $|\delta CP|=0.10$.

4.4 NMSSM

While the MSSM has been the main model for surveying the SUSY Higgs phenomenology so far, Supersymmetry may be realised in a non-minimal scenario. The introduction of an additional Higgs singlet has been proposed as a natural explanation of the value of the μ term in the MSSM Higgs potential. The resulting NMSSM Higgs sector has seven physical Higgs bosons and six free parameters. It has been shown that the prospects for

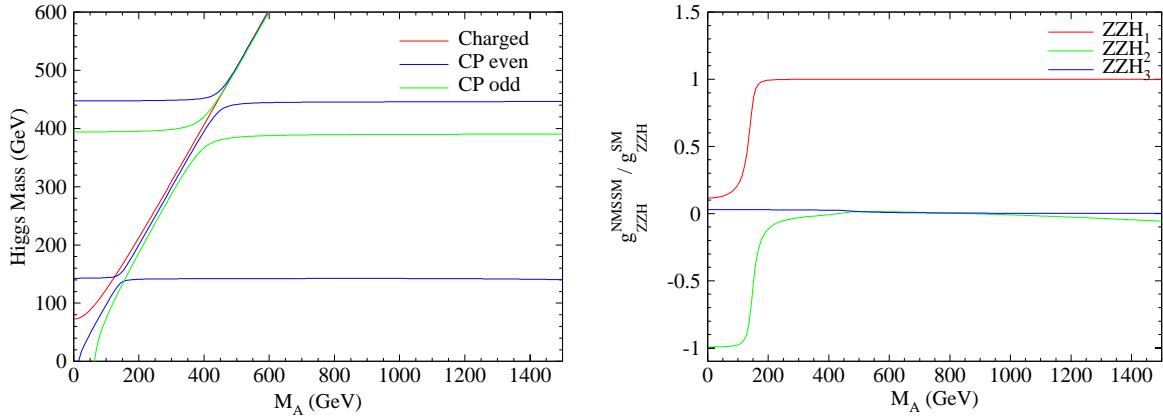


Figure 7: NMSSM Higgs masses (left) and couplings to Z^0 bosons normalised to SM value (right) as a function of M_S , for a typical set of model parameters (from [28]).

Higgs discovery at the LHC are not undermined in this scenario, provided that the full integrated luminosity of $\mathcal{L}=300$ fb^{-1} is considered [29]. This would lead to an interesting phenomenology with two scalar Higgs bosons possibly within reach of a TeV-class LC, one light pseudo-scalar and four heavy bosons almost degenerate in mass (see Figure 7) [28].

5 The Higgs Boson and the Radion in scenarios with Extra-Dimensions

The hierarchy problem, originating from the mismatch between the electroweak scale, defined by the Higgs field vacuum expectation value $v = 246$ GeV and the Planck scale, has motivated the introduction of models with hidden extra dimensions. In the original construction of the Randall-Sundrum formulation [30], the SM particles live on a brane, while gravity expands on a second, parallel brane and in the bulk. This scenario introduces a new particle, the Radion, which represents the quantum excitation of the brane separation. By mixing with the Higgs field, the Radion modifies the Higgs couplings to SM particles and thus its decay branching fractions $\text{BR}(H \rightarrow f\bar{f})$ [31, 32]. Examples are shown in Figure 8 for $M_H=125$ GeV. The typical accuracies for the branching fraction determination at the LC make these shifts significant enough to reveal the radion effects over a large fraction of the parameter space, including regions where evidence of the radions and of the extra-dimensions could not be obtained directly.

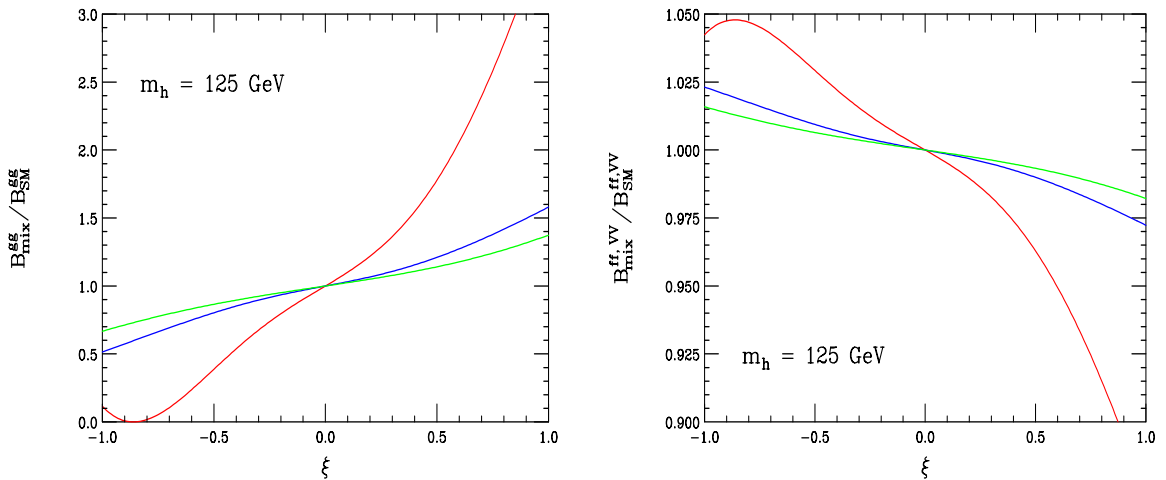


Figure 8: Modified Higgs couplings to gluons (left) and fermions and vector gauge bosons (right) induced by Radion-Higgs mixing. The effects are shown, as function of the mixing parameter, ξ , for three sets of values of the Radion mass and the Λ scale of the theory (from [31]).

6 Conclusions

The present theory of fundamental interactions and the experimental evidence strongly suggest that the electro-weak symmetry is broken via the Higgs mechanisms, while par-

ticles acquire their mass through their interaction with the scalar Higgs field. The Higgs boson is heavier than 114 GeV and possibly lighter than about 210 GeV. Within this scenario we expect the LHC to discover such Higgs boson and a high energy, high luminosity e^+e^- linear collider to accurately determine its properties. These precisions can be obtained within a realistic run plan scenario. Charting the Higgs profile will not only clarify if the Higgs mechanism is indeed responsible for electro-weak symmetry breaking and mass generation. It will also elucidate the nature of the Higgs particle. As the discovery of Hispaniola deceived Columbus on the essence of his achievement, the Higgs sector may have more and different properties than those expected in the SM or even considered in this paper. Higgs physics at the LC may thus provide the first clues on New Physics beyond the SM and possibly a new world of particles, as predicted in Supersymmetry. While most of the mapping of the lighter Higgs profile can be optimally performed at a LC with centre-of-mass energies in the range 300-500 GeV, there are measurements which will require higher energies. An upgrade of the centre-of-mass energy to $\simeq 1$ TeV and a second stage multi-TeV LC should complete the measurement of the Higgs properties with the needed accuracy and extend the sensitivity to heavier Higgs bosons, beyond the LHC reach, depending on the nature of the Higgs sector. In all cases, linear colliders add crucial information to previous data and to the data that the LHC will obtain.

It is a pleasure to thank the organisers for their invitation and for a most pleasant Conference. I am grateful to Albert De Roeck, Klaus Desch, Daniele Dominici, Jack Gunion, Joanne Hewett, Tom Rizzo, Ian Wilson, and Peter Zerwas for suggestions and discussion.

References

- [1] P.W. Higgs, *Phys. Rev. Lett.* **12** (1964) 132; *idem*, *Phys. Rev.* **145** (1966) 1156; F. Englert and R. Brout, *Phys. Rev. Lett.* **13** (1964) 321; G.S. Guralnik, C.R. Hagen, and T.W. Kibble, *Phys. Rev. Lett.* **13** (1964) 585.
- [2] M. Grünewald, to appear in the Proc. of the 31st Int. Conf. on High Energy Physics, Amsterdam, July 2002 and [arXiv:hep-ex/0210003].
- [3] *TESLA: The superconducting electron positron linear collider with an integrated X-ray laser laboratory. Technical design report.*, R. Brinkmann, K. Flottmann, J. Rossbach, P. Schmuser, N. Walker, and H. Weise (editors), DESY-01-011 and ECFA-2001-209.

-
- [4] *2001 report on the Next Linear Collider: A report submitted to Snowmass 2001*, NLC Collaboration, in *Proc. of the APS/DPF/DPB Summer Study on the Future of Particle Physics (Snowmass 2001)* ed. N. Graf, SLAC-R-571 Prepared for APS / DPF / DPB Summer Study on the Future of Particle Physics (Snowmass 2001), Snowmass, Colorado, 30 Jun - 21 Jul 2001.
- [5] M. Battaglia, I. Hinchliffe, J. Jaros, and J. Wells, in *Proc. of the APS/DPF/DPB Summer Study on the Future of Particle Physics (Snowmass 2001)* ed. N. Graf, [arXiv:hep-ex/0201018].
- [6] *A 3 TeV e^+e^- Linear Collider Based on CLIC Technology*, The CLIC Study Team, G. Guignard (editor), CERN-2000-008.
- [7] H. Braun, S. Doebert, I. Syratchev, M. Taborelli, I. Wilson, and W. Wuensch, to appear in *Proc. of the XXI International Linac Conference*, August 19-23 2002, Gyeongju (Kyongju), Korea.
- [8] P. Garcia *et al.*, LC-PHSM-2001-054; T. Abe *et al.*, [arXiv:hep-ex/0106056].
- [9] M. Schumacher, LC Note in preparation.
- [10] T. Abe *et al.* [American Linear Collider Working Group Collaboration], in *Proc. of the APS/DPF/DPB Summer Study on the Future of Particle Physics (Snowmass 2001)* ed. N. Graf, SLAC-R-570 Resource book for Snowmass 2001, 30 Jun - 21 Jul 2001, Snowmass, Colorado.
- [11] K. Desch and N. Meyer, LC-PHSM-2001-025.
- [12] M. Battaglia and D. Schulte, [arXiv:hep-ex/0011085].
- [13] M. Battaglia, in *Proc. of 4th Int. Workshop on Linear Colliders (LCWS 99)* and [arXiv:hep-ph/9910271].
- [14] J.C. Brient, Note LC-PHSM-2002-003.
- [15] C. T. Potter, J. E. Brau, and M. Iwasaki, in *Proc. of the APS/DPF/DPB Summer Study on the Future of Particle Physics (Snowmass 2001)* ed. N. Graf and *Proc. of the 6th Int. Linear Collider Workshop (LCWS2002)*, Jeju Island (Korea), 2002.
- [16] S. Dittmaier, M. Kramer, Y. Liao, M. Spira, and P. M. Zerwas, *Phys. Lett. B* **441** (1998) 383 [arXiv:hep-ph/9808433].

-
- [17] M. Battaglia and A. De Roeck, in *Proc. of the APS/DPF/DPB Summer Study on the Future of Particle Physics (Snowmass 2001)* ed. N. Graf, [arXiv:hep-ph/0111307].
- [18] A. Djouadi, W. Kilian, M. Muhlleitner, and P. M. Zerwas, *Eur. Phys. J. C* **10** (1999) 27 [arXiv:hep-ph/9903229].
- [19] C. Castanier, P. Gay, P. Lutz, and J. Orloff, [arXiv:hep-ex/0101028].
- [20] M. Battaglia, E. Boos, and W. M. Yao, in *Proc. of the APS/DPF/DPB Summer Study on the Future of Particle Physics (Snowmass 2001)* ed. N. Graf, [arXiv:hep-ph/0111276].
- [21] K. Desch and M. Battaglia, LC-PHSM-2001-053.
- [22] K. Desch and N. Meyer, LC Note in preparation.
- [23] M. Battaglia, A. Ferrari, and A. Kiiskinen, in *Proc. of the APS/DPF/DPB Summer Study on the Future of Particle Physics (Snowmass 2001)* ed. N. Graf, [arXiv:hep-ph/0111307].
- [24] A. Andreazza and C. Troncon, DESY-123-E, 417.
- [25] M. Muehleitner, in *Proc. of the 5th Int. Linear Collider Workshop (LCWS 2000)* A. Para and H.E. Fisk (editors), Melville, AIP, (2001).
- [26] M. M. Muhlleitner, M. Kramer, M. Spira, and P. M. Zerwas, *Phys. Lett. B* **508** (2001) 311 [arXiv:hep-ph/0101083].
- [27] E. Christova, H. Eberl, W. Majerotto, and S. Kraml, *Nucl. Phys. B* **639** (2002) 263 [arXiv:hep-ph/0205227].
- [28] D.J. Miller, in these proceedings.
- [29] U. Ellwanger, J. F. Gunion, and C. Hugonie, [arXiv:hep-ph/0111179].
- [30] L. Randall and R. Sundrum, *Phys. Rev. Lett.* **83** (1999) 4690 [arXiv:hep-th/9906064] and *Phys. Rev. Lett.* **83** (1999) 3370 [arXiv:hep-ph/9905221].
- [31] J. L. Hewett and T. G. Rizzo, [arXiv:hep-ph/0202155].
- [32] D. Dominici, B. Grzadkowski, J. F. Gunion, and M. Toharia, [arXiv:hep-ph/0206192].